

# CAN THE HISTORY FORCE BE NEGLECTED FOR THE MOTION OF PARTICLES AT HIGH SUBCRITICAL REYNOLDS NUMBER RANGE?

*Mohammad Rostami\* and Abdullah Ardeshir*

*Department of Civil and Environmental Engineering, Amir Kabir University of Technology  
Tehran, I. R. of Iran, m\_rostami@aut.ac.ir – aardeshir53@yahoo.com*

*Goodarz Ahmadi*

*Department of Mechanical and Aeronautical Engineering, Clarkson University  
Potsdam, NY, USA, ahmadi@clarkson.edu*

*Peter Joerg Thomas*

*Department of Engineering, University of Warwick, Coventry, UK  
Eddy.decay@eng.warwick.ac.uk*

\*Corresponding Author

(Received: May 31, 2006 – Accepted in Revised Form: November 2, 2006)

**Abstract** In the present work, the motion of metallic and plastic particles of 5 mm diameter falling in a quiescent fluid is investigated experimentally. The goal of this investigation is to examine the effect of history force acting on a particle in a range of Reynolds numbers between 1000 and 5000. The instantaneous position of the particle was recorded using a high - speed camera (500 to 1000 frames per second). The comparison is made by solving the equation of motion of particle with and without history force based on the Lagrangian approach. The results showed that the combination of gravity, drag and added mass forces are important for simulation of particle motion from the starting point of motion to the wall impact in the range of aforementioned Reynolds numbers. Nevertheless, the predicted trajectories underestimate the experimental observations. In this case, excellent agreement between the measured and predicted particle trajectory was obtained when the history force was included in the governing equation. Analysis of the results showed, however, the history force in comparison with the other hydrodynamic forces in prediction of the particle motion, from the starting point of motion to the wall impact has a small effect which is about 1 to 4.3 % and can be ignored. But it has a considerable effect on the bouncing motion of the particle after the first collision, even for the Reynolds numbers up to 5000.

**Key Words** Lagrangian Approach, Drag Force, Added Mass Force, History Force, Bouncing Motion.

**چکیده** در مقاله حاضر حرکت ذرات کروی پلاستیکی و فولادی به قطر ۵ میلیمتر در یک سیال ساکن بطور آزمایشگاهی بررسی شده است. هدف از این مقاله، بررسی اثر نیروی پیشینه وارد بر ذره در اعداد رینولدز بین ۱۰۰۰ و ۵۰۰۰ می باشد. به منظور ثبت حرکت ذرات از یک دوربین دیجیتالی سرعت بالا (۵۰۰ تا ۱۰۰۰ تصویر در هر ثانیه) استفاده گردید. سپس مسیر ثبت شده با نتایج بدست آمده از حل عددی معادله حرکت ذره به روش لاگرانژی در شرایط وجود و عدم وجود نیروی پیشینه مقایسه شده است. نتایج نشان می دهد که هرچند تلفیق نیروهای گرانشی، پسا و جرم ظاهری در شبیه سازی حرکت ذرات از نقطه شروع حرکت تا برخورد به دیواره در محدوده اعداد رینولدز فوق الذکر از اهمیت بالایی برخوردار می باشند، اما مسیر پیش بینی شده توسط نیروهای مذکور بر مسیر آزمایشگاهی منطبق نمی گردد. در این شرایط، تطابق خوب زمانی حاصل می شود که اثر نیروی تاریخی در معادله حاکم بر حرکت ذره ملحوظ گردد. تحلیل نتایج نشان می دهد که هرچند نیروی پیشینه در مقایسه با دیگر نیروهای هیدرودینامیکی در پیش بینی مسیر حرکت ذره از شروع حرکت تا برخورد به دیواره اثر کمی در حدود ۱ تا ۴/۳ درصد داشته، اما می توان آنرا نادیده گرفت. در حالیکه این نیرو در شبیه سازی مسیربرگشت ذره در اولین برخورد به دیواره، نقش بسیار قابل توجهی را حتی در اعداد رینولدز نزدیک به ۵۰۰۰ ایفا می نماید.

## 1. INTRODUCTION

The accurate evaluation of the hydrodynamic

forces acting on a particle moving in a viscous fluid remains a fundamental question in multiphase flow modeling. This problem arises in many

engineering applications, e.g., spray combustion, pollution control, boiling and bubble dynamics, sedimentation, and erosion of turbine blades. All these problems are concerned with interaction of particles with fluids, which requires accurate knowledge of all hydrodynamic forces acting on a particle. Another problem is associated with the ability of dispersed solid particles to follow the fluid motion when their density or initial velocity does not match the fluid velocity or its density; that is, the ability of solid particles to behave as Lagrangian tracers of fluid motion. This issue is of importance for the prediction of dispersion of particles in flows, as well as for measurement techniques such as particle image velocimetry (PIV). So this motivation comes from work aiming at developing a Lagrangian tracking technique for the motion of solid particles during large intervals of times. It raises the question of the response of a particle to rapid changes in the velocity of the fluid, or to a sudden acceleration. Analytical approaches to the time - dependent motion of a solid particle in a given quiescent fluid have been restricted to zero or small Reynolds numbers. However, they provide a general frame of description of the forces acting on the particle. Since the equation of particle motion in its general form is rather cumbersome to deal with. Usually various simplified versions are used. In other words, among the forces acting on a particle, the gravity force, the quasi - steady drag and the added mass force are currently included and their adequate expressions are now well defined. The history force, taking into account the vorticity diffusion in the surrounding fluid and the disturbance effect caused by the acceleration of the sphere, is often neglected in simulation of particle trajectory. Nevertheless, the applicability of the equation of motion is still to be clarified. If one considers the equation of the particle motion trajectory with parameters corresponding to the creeping flow approximation, one finds that the history force generally should exceed inertial forces.

In several papers, advection of particles with inertia in a fluid was investigated numerically under an assumption that the history force can be neglected [1-8]. Ounis and Ahmadi [9] studied the motion of small spherical particles (order of size:  $\mu\text{m}$ ) in a random flow field analytically. The equation of

motion of a small spherical rigid particle in a turbulent flow field, including stokes drag, virtual mass and the Basset (history) force effect were considered. Results obtained recently for the motion of a particle in a shock wave show that the Basset force can be even more significant than stokes drag force [10]. Abbad et al. [11,12] experimentally studied a free - falling rigid sphere in a quiescent incompressible Newtonian fluid, placed in an oscillating frame. They investigated numerically the effect of the history force acting on the sphere at small Reynolds numbers ( $Re \leq 2.5$ ). The comparison was made by solving the equation of motion of the sphere with and without the history force. They found that the history force plays a significant role in the momentum balance. Harada et al. [13] studied both experimentally and numerically a spherical nylon particle of diameters 12.7 and 25.4 mm approaching a wall in an incompressible fluid under the action of gravity at Reynolds numbers 6.01 and 25.8, respectively. Their results show that in addition to the gravity, the drag and the added mass force, the Basset history force also has a significant effect on the particle motion through the sedimentation in both cases. Gondret et al. [14] investigated both experimentally and numerically the bouncing motion of solid spheres onto a solid plate in an ambient fluid. They demonstrated that history forces cannot be neglected for the bouncing trajectories after the collisions for Reynolds numbers up to about  $10^3$ .

Most of the previous studies have been performed on the motion of particles in a quiescent fluid at low and moderate Reynolds numbers (less than 1000). The objective of the present paper is to examine the effect of the history force on the motion of spherical metallic and plastic particles at high subcritical Reynolds number. Both experiments and a numerical analysis are conducted to examine the fluid forces in a range extending from  $1000 < Re_p < 5000$ . In the present paper, we focus on the trajectory of the particles motion from the starting point to the wall impact and the first rebound trajectory as well. The particle trajectory is calculated with the Lagrangian approach. We use the equation of particle motion and take into account the corresponding condition imposed on the fluid. In our numerical model, gravity, drag, added mass and history forces are

considered with proper modification.

## 2. FORMULATION AND NUMERICAL METHOD

The particle trajectory can be determined by solving its equation of motion, which can be deduced from Newton's Second Law. The equation of motion for small particles in a viscous quiescent fluid dates back to the pioneering work of Basset, Boussinesq and Oseen, and is commonly known as the BBO equation. They solved the Navier Stokes equations for a creeping flow by neglecting the advective acceleration terms and derived the following equation for the acceleration of the sphere [15]:

$$m_p \frac{dU}{dt} = -6a\pi\mu_f U - \frac{1}{2} m_f \frac{dU}{dt} - 6a^2 \sqrt{\pi\mu_f \rho_f} \int_0^t \frac{\partial U / \partial \tau}{\sqrt{t-\tau}} d\tau + (m_p - m_f)g \quad (1)$$

Where  $\rho_f$  is the density of the fluid,  $\mu_f$  is the viscosity of the fluid,  $U$  is the sphere velocity,  $a$  is the sphere radius,  $m_p$  is the sphere mass,  $m_f$  is the mass of the fluid displaced by the sphere ( $m_f = (4/3)\pi a^3 \rho_f$ ) and  $t$  and  $\tau$  are time scales. The right hand side of Equation 1 consists of the summation of all forces exerted on the particle along its trajectory in quiescent fluid. The terms on the right-hand side of Equation 1 are, in the order of their appearance, steady drag ( $F_D$ ), apparent or added mass force ( $F_A$ ), Basset or history force ( $F_H$ ) and gravity force which is divided into the weight of the body owing to its mass and the buoyancy ( $F_G$ ).

The steady drag is responsible for the terminal velocity of a sphere falling under gravity. The expression in Equation 1 is valid only for  $Re_p = 0$  ( $Re_p = 2aU\rho_f/\mu_f$ ). It is well known that for finite Reynolds numbers, the convective inertia increases the drag. The analytic expression is not known for all Reynolds numbers but the empirical law for the drag coefficient as a function of  $Re$  is well documented for a noncreeping flow from  $Re_p \rightarrow 0$  up to values higher than  $10^7$ . One usually writes the steady drag as:

$$F_D = -6a\pi\mu_f U \varphi \quad (2)$$

Where  $\varphi$  is a function of the Reynolds number. Various approximations of  $\varphi$  ( $Re_p$ ) for rigid spherical particles can be found in the book of Clift et al. [16]. In the present study we used the following approximation of the  $\varphi$  ( $Re_p$ ) valid in a wide range of Reynolds numbers [17]:

$$\varphi = (1 + 0.15 Re_p^{0.687}) + \frac{1.75 \times 10^{-2} Re_p}{1 + 4.25 \times 10^4 Re_p^{-1.16}} \quad (3)$$

$$Re_p < 3 \times 10^5$$

The second term in Equation 1 is the added mass force which is found to be in the two limit cases of creeping and inviscid flows [18]. Recent numerical studies show that the added mass term for finite - Reynolds - number flows is the same as predicted by creeping flow and potential flow theory over a wide range of the dimensionless relative acceleration [19]. Odar and Hamilton [20] and Odar [21] studied experimentally the force on a guided sphere rectilinearly oscillating in an otherwise stagnant fluid. The expression of Odar and Hamilton modifying the Added mass force just by a numerical coefficient to account for the inertial effect at high Reynolds numbers as follow:

$$F_A = -\frac{1}{2} C_a m_f \frac{dU}{dt} \quad (4)$$

where  $C_a$  obtained experimentally and given by:

$$C_a = 2.1 - \frac{0.132}{A_c^2 - 0.12} \quad (5)$$

The parameter  $A_c$  is called the acceleration number and is defined by:

$$A_c = \frac{2U^2}{a|dU/dt|} \quad (6)$$

Note that in the inviscid limit, the added mass

force is modified by the presence of a wall by the factor  $(1 + 3a^3/8(a+h)^3)$ , where  $h$  is the distance of the bottom apex of the particle from the wall [18]. This modification is not so large since this factor never exceeds 11/8. As we do not see a significant effect on the trajectory before and after the collision, we will neglect this factor in the following and thus assume that the added - mass force is given by Equation 4. The third term in Equation 1 is the history force which may be expressed as:

$$F_D = -6a\pi\mu_f \int_{-\infty}^t K(t,\tau, Re_p)(\partial U/\partial \tau) d\tau \quad (7)$$

Where it appears as a convolution product of the acceleration of the particle with the kernel  $K(t, s; Re_p)$ . At zero Reynolds number, the history term is known as the Basset force with the kernel  $K(t, \tau) = \left[ \rho_f a^2 / \pi\mu(t-\tau) \right]^{1/2}$  as shown in Equation 1. At nonzero Reynolds number, the kernel expression for the history force is still controversial. In this study, for the simulation of particle trajectory since their start to the wall impact we have chosen the expression of Odar and Hamilton as the following equation which is modifying the Basset force just by a numerical coefficient at high Reynolds numbers [20,21]:

$$F_H = -6a\pi\mu_f C_h \int_{-\infty}^t \left[ \rho_f a^2 / \pi\mu(t-\tau) \right]^{1/2} (\partial U/\partial \tau) d\tau \quad (8)$$

Where also  $C_h$  obtained experimentally in the following form:

$$C_h = 0.48 - \frac{0.32}{(A_c + 1)^3} \quad (9)$$

In the numerical calculation of the particle motion, the main problem is solving the Equation 8. We assumed that the general temporal variation of particle velocity can be broken up into a series of step changes. At time 0 there is a change  $\Delta U_0$ , at time  $t_1$  a change  $\Delta U_1$  and at time  $t_2$  a change  $\Delta U_2$

and so on. For instance, to compute the effect of history force at time  $t_3$  with a constant time step  $\Delta t$ , the cumulative effect of the history force can be written as follow:

$$F_{H_{t_3}} = -6a^2 C_h \sqrt{\pi\mu_f \rho_f} \int_0^{t_3} \frac{\partial U/\partial \tau}{\sqrt{t-\tau}} d\tau = -6a^2 C_h \sqrt{\pi\mu_f \rho_f} \left[ \frac{\Delta U_0}{\sqrt{t_3}} + \frac{\Delta U_1}{\sqrt{t_3-t_1}} + \frac{\Delta U_2}{\sqrt{t_3-t_2}} \right] \quad (10)$$

More recently, the analysis of Lawrence and Mei [22] has shown that the asymptotic behavior of the kernel at long times may be  $t^{-2}$  or  $t^{-1}$  or even exponential, depending on the type of motion (sudden stop, sudden increase, reverse motion ...). The exceptional case occurs for reversed motion which the particle interacts directly with its wake. To show this effect, they took into account the modification of the wake of the particle due to the modification of the motion. Very little visualization of the fluid mechanics due to the impact of the bodies on surfaces and bouncing motion has been undertaken. The recent article by Thompson et al. [23] just showed that when a cylinder collides normally to the wall and stick, two vortices are produced from its wake that diverts from the particle. As it is evident from Figure 1, the wake at upstream of the cylinder will decay after a time that depends on the Reynolds number. But, if the body rebounds from the wall and experiences a bouncing motion with a constant velocity  $U_r = eU_i$  ( $e$  is restitution coefficient) imposed after an initial constant velocity  $U_i$ , this means that the body has to pass through its own old wake. By this kind of motion, Lawrence and Mei obtained analytically the following expression for the history force on a body to accounts the effect of its old wake:

$$F_H = -6a\pi\mu_f U_r \varphi_H(t) \quad (11)$$

where,

$$\varphi_H(t) \sim \frac{3}{2} (\varphi_r + Re_{pr} \varphi_r') \frac{\alpha_{ri}}{1 + \alpha_{ri}} \varphi_i T^{-1} \quad (12)$$

Where  $\varphi_r$  and  $\varphi_i$  are abbreviated for  $\varphi(Re_{pr})$  and

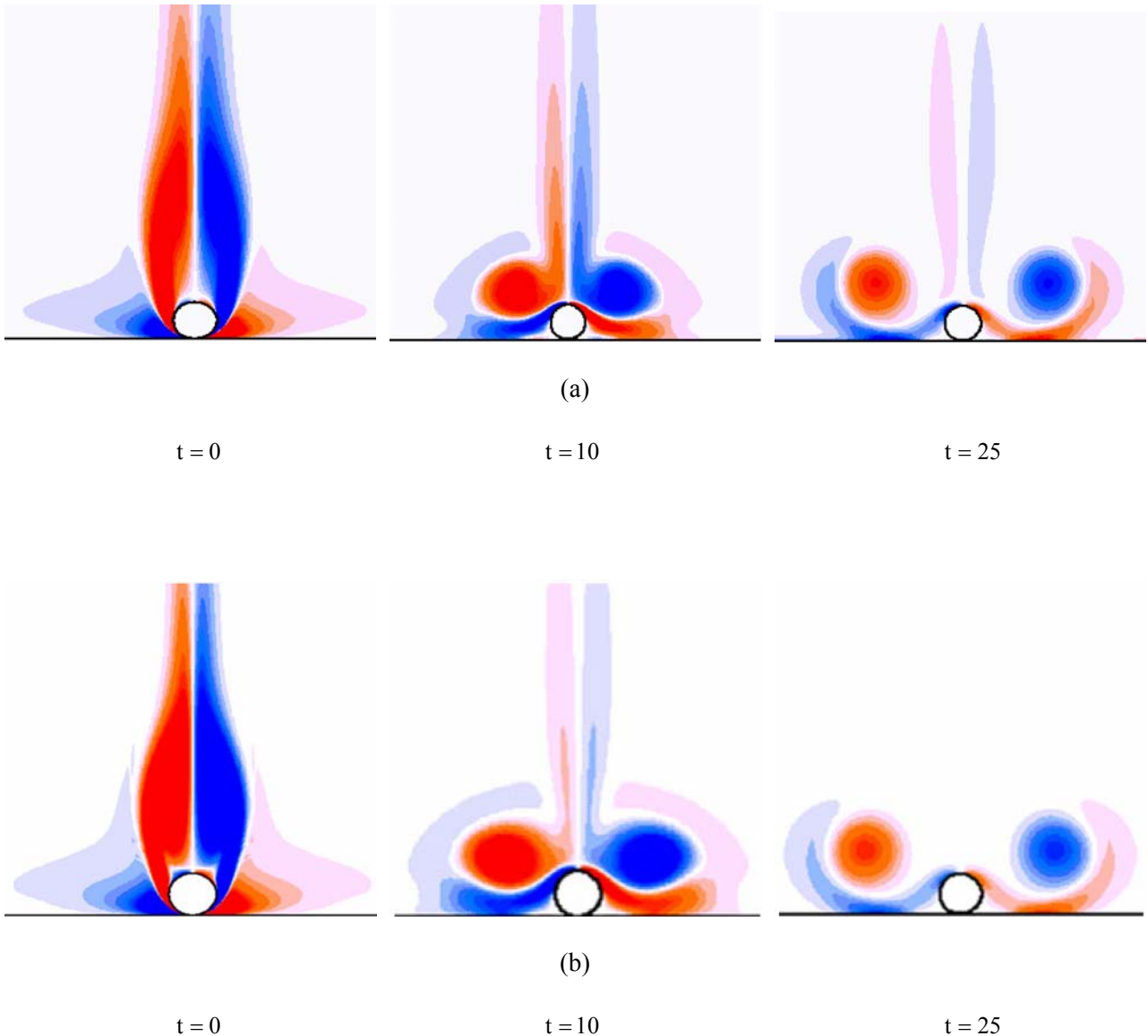


**Figure 1.** Vorticity contour plots showing the evolution of the vorticity during impact and afterwards as the initially trailing wake overtake the cylinder and interacts with the wall. The Reynolds number is (a) 100 and (b) 200. ( $t = t U_i/a$  is a dimensionless time).

$\varphi$  ( $Re_{p_i}$ ) as defined in Equation 3, respectively,  $\varphi'$  is the derivative of  $\varphi$  with respect to  $Re_p$ ,  $\alpha_{ri} = |U_i/U_r|$  is a dimensionless factor and  $T = tU_r/a$  is a dimensionless time. According to Equation 12, the reverse motion of particle onto its own old wake leads to a smaller decrease of the history

force by an amount which scales with  $t^{-1}$ . In this study, we have chosen Equation 11 to take this history term in our calculations for the simulation of rebound trajectories.

In this article, the velocity of a particle is obtained by integrating Equation 1 using the

Runge - Kutta 4<sup>th</sup> order method and the particle position is determined according to the velocity ( $U = dx/dt$ ).

### 3. EXPERIMENTAL SET - UP

The trajectory of solid particles motion since their start to the wall impact and then the first rebound trajectory are investigated experimentally. We used solid spheres made of different materials and with the same diameter. The experiments were conducted by dropping the particles in water. The mass density of water is 998.1 (kg/m<sup>3</sup>), whereas the viscosity is  $1 \times 10^{-3}$  Pas (at T = 20° Celsius). The particle trajectory is recorded by a high speed camera (Photron Fastcam PC1 1024) at 500 and 1000 frames per second. The recorded sequences of the particle motion are analyzed by using the Photron Fastcam Viewer. The experiments were conducted in a rectangular Plexiglas tank with base dimensions of 275 mm × 275 mm and a depth of 280 mm. To avoid air entertainment, the particles were initially submerged and held in a place a few millimeters under the water surface by means of a suitable support. Table 1 summarizes the relevant properties of the spheres used in this study. Figure 2 depicts the sequences of snapshots of the motion of different particles onto the wall in water.

### 4. RESULTS AND DISCUSSIONS

In Section 4.1, to examine the history force effect

on the motion of the particles from the starting point of falling motion ( $t, U = 0$ ) to the wall impact ( $t_i, U_i$ ), Equation 1 contain the drag force Equation 2, the added mass force Equation 4, the history force Equation 8 and the gravity force as shown in Equation 1 is solved with and without the history force and the results obtained are compared to the experimental observations. In Section 4.2, we present and discuss some preliminary results about the first rebound trajectories of the spheres. The equation of motion of the particle after wall impact is the same as the equation which was used in Section 4.1 with a difference that the history force is evaluated by Equation 11 to account the history effect of the old wake. It should be noted that the initial rebound velocity ( $U_r$ ) which is used for the calculations in Section 4.2 is the experimental one (see Table 1).

#### 4.1. Trajectory From Initial Motion of Particle to the Wall Impact

In this section, the results of experimental and numerical modeling of the trajectory and the velocity of the particles falling from rest toward a horizontal wall in water are investigated. Figure 3 displays the experimental and numerical trajectories of the Delrin sphere. As the figure shows, our experimental data are very close to those obtained by solving Equation 1 including the history force. We observe that by neglecting this force, the sphere trajectory will be underestimated as the figure shows. The results analysis shows that the combination of the gravity, the drag and the added mass forces can explain up to about 95.7 percent of the experimental data. Therefore, the addition of these terms is not sufficient to produce the

TABLE 1. Properties of the Particles and Experimental Conditions in this Study.

| Particle Type | $\frac{\rho_p}{\rho_f}$ | $2a$ (mm) | $h_0$ Falling height (mm) | $U_i$ Impact velocity (m/s) | $U_r$ Rebound velocity (m/s) | $t_i$ Bed impact time (s) | $Re_p$ ( $2aU_i\rho_f/\mu_f$ ) | Remarks        |
|---------------|-------------------------|-----------|---------------------------|-----------------------------|------------------------------|---------------------------|--------------------------------|----------------|
| Delrin        | 1.62                    | 5         | 195                       | 0.215                       | 0.157                        | 1.02                      | 1040                           |                |
| Teflon        | 2.30                    | 5         | 195.5                     | 0.409                       | 0.295                        | 0.566                     | 1925                           |                |
| Steel         | 7.79                    | 5         | 195.7                     | 1.049                       | 0.868                        | 0.273                     | 4670                           |                |
|               | 7.8                     | 3         | 500                       | 0.810                       | -                            | 0.649                     | 2700                           | Reference [24] |
|               | 7.7                     | 4         | 500                       | 0.970                       | -                            | 0.597                     | 4300                           |                |

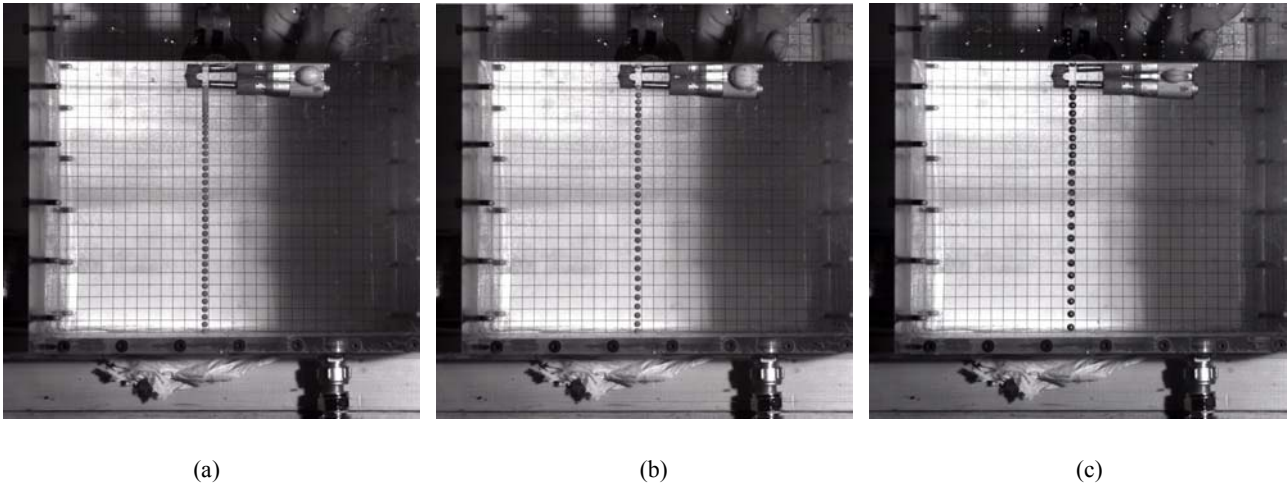


**Figure 2.** Experimental facility and pictures of the particle motion toward a Plexiglas plate from in water.  
 (a) Delrin particle, (b) Teflon particle and (c) Steel particle.

experimental data, which clearly shows that the history force is necessary. However, the effect of this force (about 4.3 percent) is weak and just results in a slight correction. In this case, the particle Reynolds number ( $Re_p$ ) based on the impact velocity is about 1040. Another attempt to examine the influence of history force on the motion of the Delrin particle in water is shown in Figure 4 where the velocity profile for each case from the numerical simulation is compared to the experimental velocity profile. These curves provide clear information about the slight effect of the history force on the motion of the Delrin particle. Here, an excellent agreement is observed when the history force is taken into account.

By choosing the Teflon particle and changing the value of density from 1360 to 2300  $kg/m^3$ , we vary the ratio of inertia to gravitational mass and we expect to observe different dynamical behaviors. In particular, we expect the motion of a lighter bead (Delrin) to be more influenced by the eventual unsteadiness of its wake. Figure 5 shows the trajectory and velocity profile of the Teflon sphere. As it is evident from these figures, taking the gravity, the dissipating role of the drag force and added mass into account explains up to about 97.0 percent of the experimental data. But there is still a little discrepancy between the experimental

and numerical results. Therefore, in this case a good agreement is again observed when the history force is not neglected even at  $Re_p \approx 1925$ . However, in this case, the history force acting on the particle is about 3.0 percent of the hydrodynamic force.

For increasing Reynolds number, we use the steel particle. The experimental and numerical trajectory and velocity profile of the steel sphere at  $Re_p \approx 4670$  is displayed in Figure 6. The results show that in spite of neglecting the history term in calculation, the major part of experimental data can be described with the other terms. However, the figure confirms that to a precise fit of the experimental trajectory, the history force effect appears again necessary but not considerable. In this case, the results obtained from numerical simulation without the history force explain up to about 99 % of the experimental data.

In the following, we have summarized the contribution of hydrodynamic forces obtained from numerical simulation on prediction of the correct particle trajectory with respect to the particle Reynolds number (Figure 7). This figure provides that for simulation of particle motion in a viscous fluid at Reynolds numbers between 1000 and 5000, the combination of gravity, drag and added mass forces become important and the history force

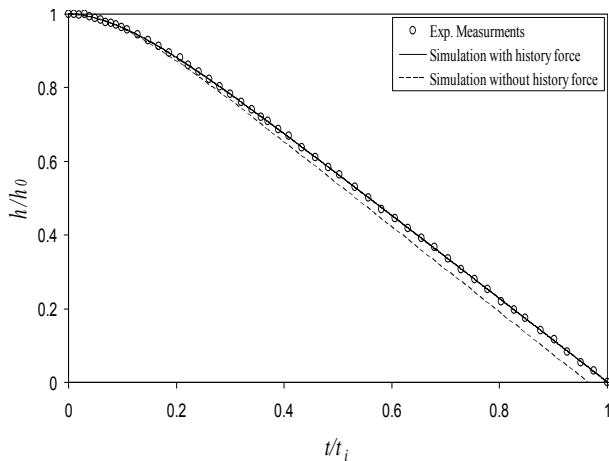


**Figure 3.** Trajectory for the motion of Delrin particle in water at  $Rep \approx 1040$  (Note:  $h$  is the distance of the bottom apex of the sphere to the wall).

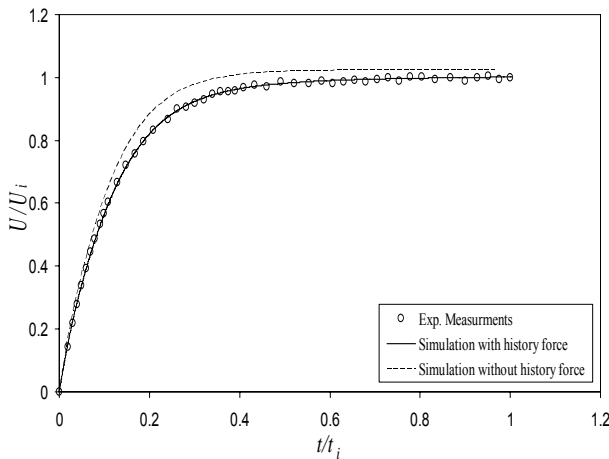


**Figure 4.** Velocity profile for the motion of Delrin particle in water at  $Rep \approx 1040$ .

effect becomes minor and just results in a slight improvement while the particle Reynolds number increases.

Finally, to verify the numerical model with and without the history force effect, the obtained solutions for the motion of steel particles of diameter 3 and 4 millimeter in water are compared with the experimental data of Mordant and Pinton [24]. From Figure 8, the good agreement between numerical and experimental results reveals the high

accuracy of the model at high subcritical Reynolds numbers when the history term is included.

**4.2. Trajectory of Bouncing Motion** In this section, we present experimental and numerical modeling of the first rebound trajectory (after the collision) of particles in water for different density ratio and different Reynolds numbers. The case of a Delrin sphere with 5 mm diameter is displayed in Figure 9 for approximately  $Rep \approx 1040$  (based on the impact velocity,  $U_i$ ). As shown in Figure 9, taking only the gravity into account leads to a large overestimate of the rebound trajectory in comparison to that obtained in experiment. On the contrary, with the addition of the drag force to the gravity leads to an underestimate of the experimental rebound trajectory. In this case, the added mass effect turns out to be non-negligible. This force arises from the fact that, as the body accelerates through the fluid, the fluid itself must accelerate. This causes the body to behave as though it were more massive than if it were accelerating in a vacuum. The amount that the body appears to exceed its “in vacuum” mass is referred to as the “added mass”. Therefore, the added mass force is necessary to be considered. However, in this case, the addition of this term to the gravity and the drag forces is not sufficient to reproduce the experimental curve and pushes up the simulated trajectory (---) above one simulated with gravity alone (---). Analysis of the results is shown the trajectories calculated in the case where only the gravity is taken into account, or the gravity and the drag are combined and or put the gravity, the drag and the added mass forces together leads to a discrepancy around 20, -13 and 37 percent, respectively, between the experimental and the numerical apex. The addition of history force and taking into account the history effect of the old wake leads to a deviation of about 1.2 %.

The case of a Teflon sphere with 5 mm diameter is displayed in Figure 10 for approximately  $Rep \approx 1925$ . From the figure, the trajectories calculated in the case where only the gravity is taken into account, or the gravity and the drag are combined and or put the gravity, the drag and the added mass forces together leads to a discrepancy around 43, 10 and 34 percent,

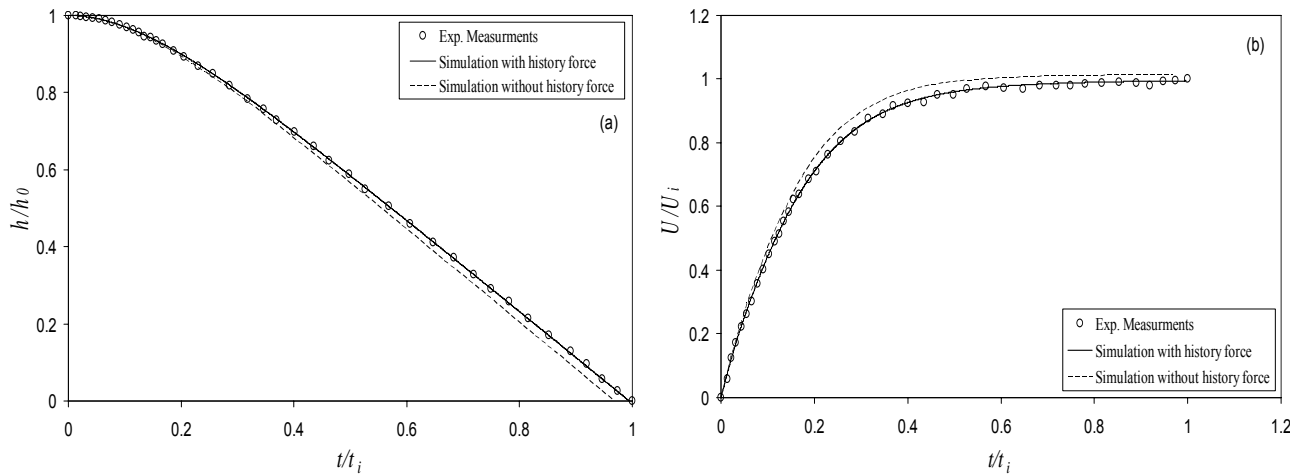


**Figure 5.** (a) Trajectory and (b) velocity profile for the motion of Teflon particle in water at  $Rep \approx 1925$ .

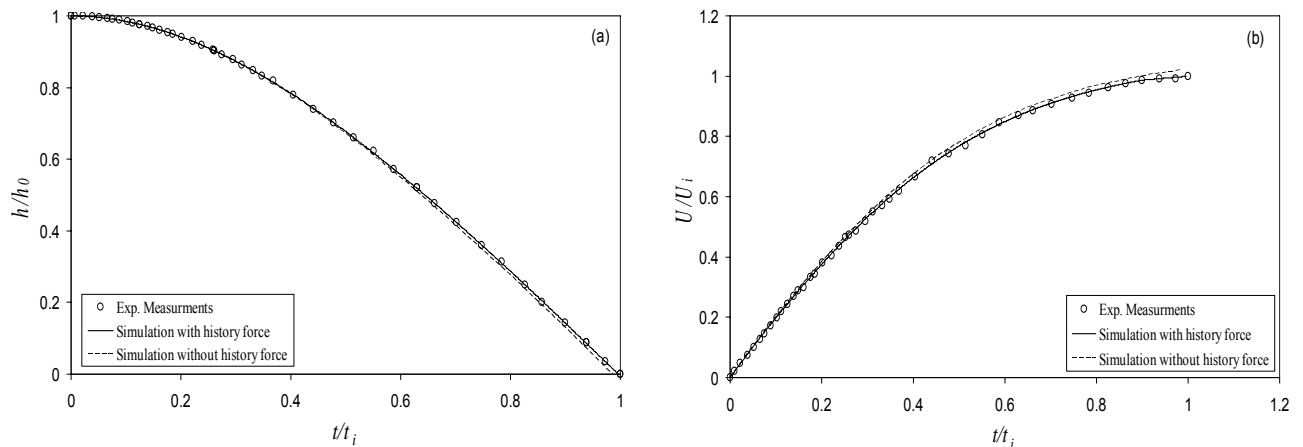


**Figure 6.** (a) Trajectory and (b) velocity profile for the motion of Steel particle in water at  $Rep \approx 4670$ .

respectively, between the experimental and the numerical apex. The addition of history force and taking into account the history effect of the old wake leads to a deviation of about 0.4 %.

The results of evaluation of hydrodynamic forces acting on a steel sphere of 5 mm diameter are shown in Figure 11 for approximately  $Rep \approx 4670$ . Comparing the experimental apex and that obtain with numerical model in the case where only the gravity is taken into account leads to a

discrepancy around 31 %. The addition of drag force reduces this wide disagreement to a value about 5 % but it is not sufficient. The added mass effect turns out to be non - negligible even for a density ratio of about 8. However, the addition of this term is not sufficient to reproduce the experimental curve, so that the trajectory simulated lies between two last simulated trajectories (FG,FG+FD). In this case, the difference between the observation and the

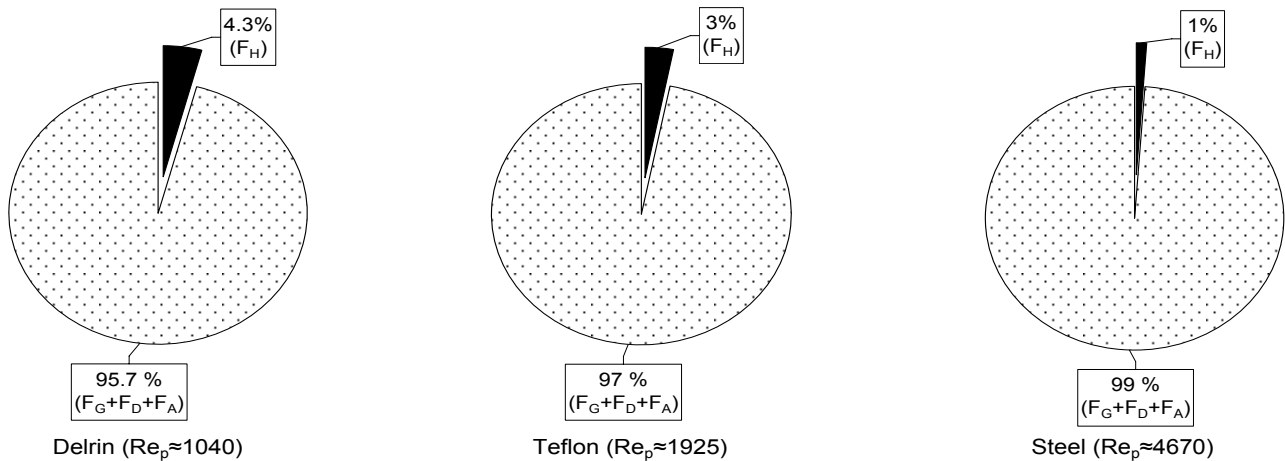


**Figure 7.** Contribution of hydrodynamic forces on prediction of the correct trajectory of different particles with respect to the particle Reynolds number in water.

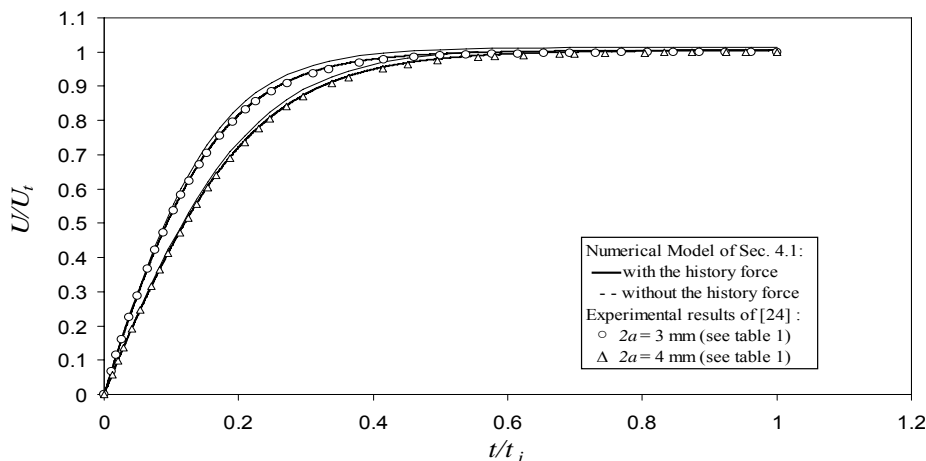


**Figure 8.** Velocity profiles of steel particles motion in water at rest. The experimental data of Reference 24 are compared with the results of the numerical model of Section 4.1.

calculation apex is about 9 %. Therefore, the history effect appears again necessary to predict the correct trajectory. The addition of this effect to the numerical model gives a rebound trajectory with excellent agreement to the observation curve.

In the three Figures 9 through 11, the curve fits of the experimental trajectories with the history term are correct but not perfect. It may be that the rebound motion is a reverse motion at a non - constant velocity (the velocity decreases with time in the first part of the rebound) contrarily to the

analysis of Lawrence and Mei [22] in which the velocity assumed to be constant. As a consequence, the time dependence of the history term will be different.

## 5. CONCLUSIONS

In the literature, there are many experimental studies on the effect of history force acting on particle motion at Reynolds numbers less than

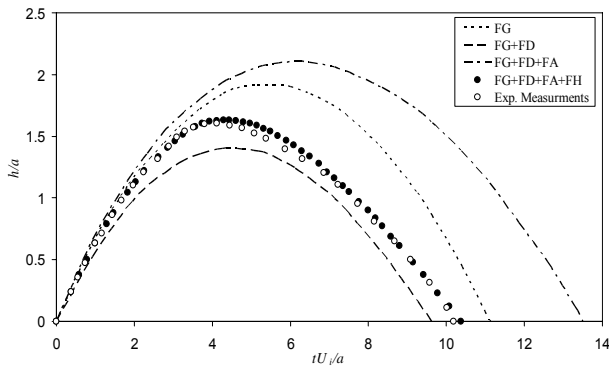


**Figure 9.** Experimental and simulation rebound trajectories for the Delrin particle at  $Re_p \approx 1040$ .

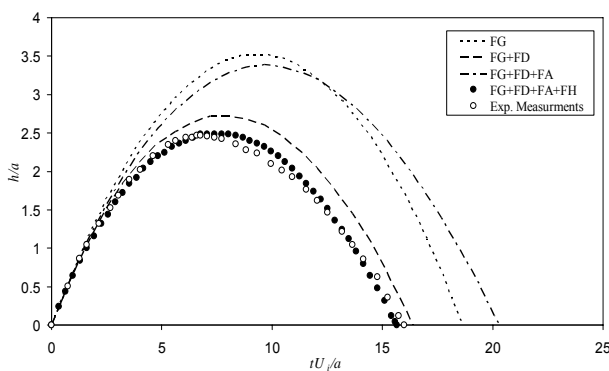


**Figure 10.** Experimental and simulation rebound trajectories for the Teflon particle at  $Re_p \approx 1925$ .

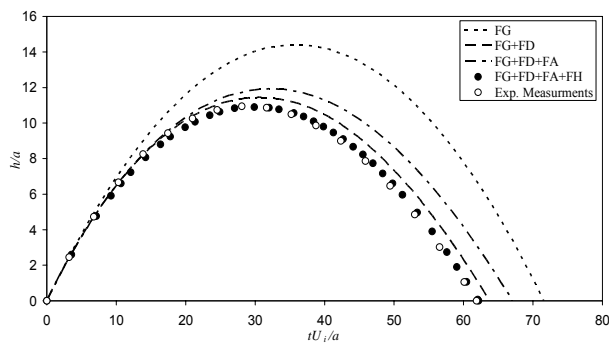


**Figure 11.** Experimental and simulation rebound trajectories for the Steel particle at  $Re_p \approx 4670$ .

1000 [10-14]. Thus, it appeared to us very useful to quantify experimentally and numerically the effect of this force on the particle motion at upper Reynolds numbers. For this, experiments were carried out to study the free motion of spherical

particle of 5mm diameter and different material (Delrin, Teflon and Steel) in the laboratory of engineering department of University of Warwick. By using a high video tracking technique and image processing software, accurate measurements of the particle position and velocity were carried out. The results showed that in water and where the Reynolds number of the particle was in the range of 1000 and 5000, the history effect turned out to be smaller when the Reynolds number was higher. Analysis the results indicated that the history force in comparison with the other hydrodynamic forces in prediction of the particle motion, from the starting point of motion to the wall impact has a small effect which is about 1 to 4.3 % and can be ignored. But it has a considerable effect on the bouncing motion of the particle after the first collision, even for the Reynolds numbers up to 5000.

## 6. ACKNOWLEDGMENTS

The authors acknowledge the financial support given by the Ministry of Education of IRAN and all the support offered by the Engineering Department of University of Warwick. The authors are also particularly indebted to Graham Canham who assisted with the performing the photography.

## 7. NOMENCLATURE

|           |  |
|-----------|--|
| $F_D$     | Drag force, [N]  |
| $F_A$     | Added mass force, [N]                                    |
| $F_H$     | History force, [N]                                       |
| $F_G$     | Gravity force, [N]                                       |
| $\rho_f$  | Density of fluid, [ $\text{kg}/\text{m}^3$ ]             |
| $\rho_s$  | Density of sphere (particle), [ $\text{kg}/\text{m}^3$ ] |
| $\mu_f$   | Dynamic viscosity of the fluid, [Pa. s]                  |
| $U$       | Sphere velocity, [m/s]                                   |
| $a$       | Sphere radius, [m]                                       |
| $m_p$     | Mass of sphere, [g]                                      |
| $m_f$     | Mass of fluid displaced by sphere, [g]                   |
| $g$       | Acceleration due to gravity, [ $\text{m}/\text{s}^2$ ]   |
| $t, \tau$ | Time scales, [s]   |
| $Re_p$    | Particle Reynolds number                                 |

|                           |  |
|---------------------------|--|
| $\varphi$                 | Function of the Reynolds number                            |
| Ca                        | Added mass force coefficient                               |
| $C_h$                     | History force coefficient                                  |
| $A_c$                     | Acceleration number  |
| h                         | Distance of the bottom apex of particle to the wall [m]    |
| $U_r$                     | Rebound velocity [m/s]                                     |
| $U_i$                     | Impact velocity [m/s]                                      |
| e                         | Restitution coefficient                                    |
| $K(t, s, Re_p)$           | History Kernel   |
| $\varphi_r, \varphi_i$    | Abbreviation for $\varphi(Re_{Pr})$ and $\varphi(Re_{Pi})$ |
| $\varphi'$                | Derivative of $\varphi$ with respect to $Re_p$             |
| $\alpha_{ir} =  U_i/U_r $ | Dimensionless factor                                       |
| $T = tU_r/a$              | Dimensionless time   |

## 8. REFERENCES

- Barnoky, G. and Davis, R. H., "Elastohydrodynamic collision and rebound of spheres: Experimental verification", *Phys. Fluids*, Vol. 31, (1988), 1324.
- Brush, R. M., Ho, H. W. and Yen, B. C., "Accelerated motion of a sphere in a viscous fluid", *J. of Hydraulics Division*, ASCE, HY1, Proceeding paper, Vol. 90, (1964), 3764.
- Gruttola, S. D., Boomsma, K., Poulikakos, D. and Ventikos Y., "Computational simulation of the blood separation process", *Artificial Organs*, Vol. 29, No. 8, (2005), 665-674.
- Hu, Z., Luo, X. and Luo, K. H., "Numerical simulation of particle dispersion in a spatially developing mixing layer", *Theoret. Comput. Fluid Dynamics*, Vol. 15, (2002), 403-420.
- Ling, W., Chung, J. N., Troutt, T. R. and Crowe, C. T., "Direct numerical simulation of a three - dimensional temporal mixing layer with particle dispersion", *J. Fluid Mech.*, Vol. 358, (1998), 61-85.
- Marchioli, C. and Soldati, A., "Mechanisms for particle transfer and segregation in a turbulent boundary layer", *J. Fluid Mech.*, Vol. 468, (2002), 283-315.
- Raju, N. and Meiburg, E., "Dynamics of small, spherical particles in vortical and stagnation point flow fields", *Phys. of Fluids*, Vol. 9, No. 2, (1997), 299-314.
- Wang, Q., Squires, K. D. and Wang, L. P., "On the effect of nonuniform seeding on particle dispersion in two - dimensional mixing layers", *Physics of Fluids*, Vol. 10, (1998), 1700-1714.
- Ounis, H. and Ahmadi, G., "Analysis of dispersion of small spherical particles in random velocity field", *Trans of the ASME*, Vol. 112, (1990), 114-120.
- Thomas, P. J., "On the influence of the Basset history force on the motion of a particle through a fluid", *Phys. of Fluids A*, Vol. 4, No. 9, (1992), 2090-2093.
- Abbad, M., Caballina, O. and Souhar, M., "Memory effect on spherical particles at low and intermediate Reynolds numbers", Advances in the modeling methodologies of two - phase flows, Lyon, France (2004).
- Abbad, M., Caballina, O. and Souhar, M., "Experimental investigation on the history force acting on oscillating fluid spheres at low Reynolds number", *Physics of Fluids*, Vol. 16, (2004), 3808-3817.
- Harada, S., Tanaka, T. and Tsuji, Y., "Fluid force acting on a falling particle toward a plane wall", *Proceeding of ASME FEDSM'00*, Boston, Massachusetts, (2000).
- Gondret, P., Lance, M. and Petit, L., "Bouncing motion of spherical particles in fluids", *Phys. of Fluids*, Vol. 14, No. 2, (2002), 643-652.
- Tchen, C - M., "Mean value and correlation problems connected with the motion of small particles suspended in a turbulent fluid", PhD thesis, Delft Univ. of Technology, the Netherlands, (1947).
- Clift, R., Grace, J. R. and Weber, M. E., "Bubbles, Drops, and Particles", Academic Press, New York, NY, (1978).
- Crowe, C., Sommerfeld, M. and Tsuji, Y., "Multiphase Flows with Droplets and Particles", CRC Press, Boca Raton, (1998).
- Millne - Thomson, L. M., "Theoretical hydrodynamics", Macmillan Education, London, (1968).
- Kim, I., Elghobashi, S. and Sirignano, W. A., "On the equation for spherical - particle motion effects of Reynolds and acceleration numbers", *J. Fluid Mech.*, Vol. 367, (1998), 221-253.
- Odar, F. and Hamilton, W. S., "Forces on a sphere accelerating in a viscous fluid", *J. Fluid Mech.*, Vol. 18, (1964), 302-314.
- Odar, F., "Verification of the proposed equation for calculation of the forces on a sphere accelerating in a viscous fluid", *J. Fluid Mech.*, Vol. 25, (1966), 591-592.
- Lawrence, C. J. and Mei, R. M., "Long - time behaviour of the drag on a body in impulsive motion", *J. Fluid Mech.*, Vol. 283, 307, (1995).
- Thompson, M., Leweke, T., Cheung, A. and Hourigan, K., "Hydrodynamics of a body impact on a wall", third international conference on CFD in the mineral and process industries, Melbourne, Australia, (2003).
- Mordant, N. and Pinton, J - F., "Velocity measurement of a settling sphere", *Eur. Phys. J. B.*, Vol. 18, (2000), 343-352.